Communication

R. M. DeSantis
Electrical and Computer Engineering Department
Ecole Polytechnique de Montréal
Montreal, Quebec, Canada, H3C 3A7

Path-tracking for a Tractor-Trailer–like Robot

Abstract

Path-tracking controllers for tractor-trailer–like robots are designed by generalizing the geometric path-tracking approach currently adopted for car-like robots. This is done by formalizing the concepts of speed and lateral and heading offsets and by assuming slippage-free motion. The main result is that for straight-line or circular-arc paths to be tracked with a constant velocity, path-tracking may be ensured by means of a linear, time-invariant, and decoupled controller, the gains of which may be determined using familiar proportional-integral-derivative (PID) and state-feedback techniques.

1. Introduction

While appropriate for many practical applications, most of the results concerning path-tracking controllers for mobile wheeled robots are of an ad hoc nature and are limited to car-like robots, straight-line paths, and a constant tracking velocity (Anderson 1985; Cox and Wilfong 1990; Giralt 1988; Borenstein and Koren 1987; DeSantis and Hurteau 1990; Lee 1992). Recently, the search for greater flexibility of motion, a greater payload, and a greater variety of vehicle formations has created an interest in extending these results into a context in which more general path assignments may be considered and the car-like robot replaced with an articulated robot (in particular, a tractor-trailer–like robot).

Typical of efforts addressing this problem is the paper by Sampei et al. (1991), which gives a systematic procedure for the design of a path-tracking controller for a tractor-trailer–like robot. Basic elements of this procedure are a slippage-free motion, a purely kinematic model of the vehicle, straight-line paths to be followed with a constant velocity, exact and Lyapunov linearizations, and time-scale transformation techniques. Similar contributions based on the same techniques propose more general and more rigorous procedures applicable to a larger class both of path assignments and articulated vehicles (Kanayama et al. 1990; Walsh et al. 1992; D'Andrea-Novel et al. 1992).

A common feature of these developments is a state-trajectory–following approach whereby the path-tracking controller is required to ensure the convergence of the vehicle's state to a desired state that is itself a prescribed function of time. While mathematically elegant and producing many interesting results, state-trajectory following may not necessarily be the best approach for designing path-tracking controllers. Indeed, the approach that is routinely adopted in industrial car-like robots (and that is based on the notion of geometric path tracking) appears to lead to simpler controllers that are more intuitive and easier to implement. This approach, traditional in automotive applications, still entails the convergence of the vehicle's state to a prescribed state. However, instead of being a preassigned function of time, this prescribed state is now a function of the configuration of the vehicle with respect to the path to be tracked (Fenton et al. 1976; Hemami et al. 1992; Shin et al. 1992).

Based on these observations, it is of interest to explore the design of path-tracking controllers for tractor-trailer–like robots by adopting the geometric path-tracking approach. We will carry out such an extension here by using a configuration space setting (Latombe 1991; Fernandez, Gurvitz, and Li 1991), by formalizing the notions of speed and lateral and heading offsets, and by assuming slippage-free motion (Alexander and Maddocks 1988).

2. Vehicle's Dynamic Model

Consider a tractor equipped with two rear-drive wheels and two front-steering wheels, linked to a trailer with two rear wheels by means of a revolute vertical joint (Fig. 1). Assume the vehicle's motion to be planar, the geometric kinematic and dynamic properties of both the tractor and the trailer to be symmetrical with respect to their longitudinal axes, and the contact between the tires and the surface to be pointwise. Assume further that the difference between the orientation of the tractor and that of its front wheels (*steering angle*)

The International Journal of Robotics Research,
Vol. 13, No. 6, December 1994, pp. 533–544,
© 1994 Massachusetts Institute of Technology.

Downloaded from ijr.sagepub.com at ARIZONA STATE UNIV on August 14, 2016

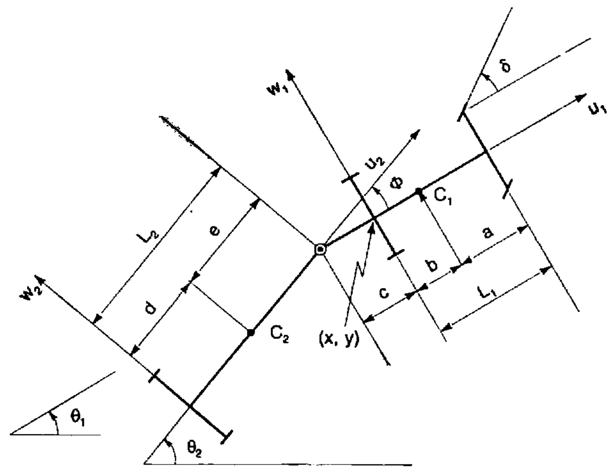

Fig. 1. Vehicle geometry.

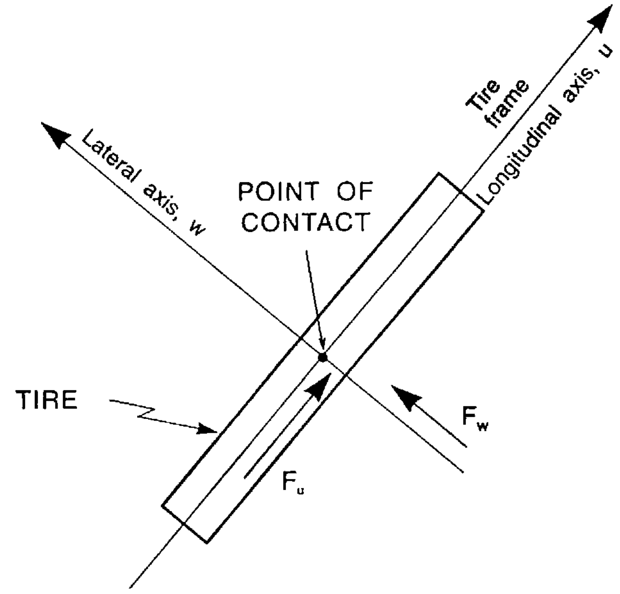

Fig. 2. Longitudinal and lateral forces exerted by the tires.

is sufficiently small that these wheels can be represented in terms of a "median" wheel located at the center of the front axle. The center of the tractor's rear axle will be referred to here as the vehicle's *guide point*.

To discuss the vehicle's dynamics we introduce the following notations (see Fig. 1):

(x, y): Workspace coordinates of the tractor's guide point.

θ_1, θ_2: Tractor's, trailer's heading.

Φ: Trailer's orientation with respect to the tractor.

δ: Steering angle.

v_u, v_w: Velocity of the tractor's center of mass (c.o.m.) in tractor-frame coordinates.

Ω_1, Ω_2: Angular velocities of the tractor and the trailer.

$\mathbf{F}_u$: Three-dimensional vector, the entries of which describe the longitudinal forces exerted by the tires on the vehicle (Fig. 2).

f_p: Propulsion control.

f_s: Steering control.

b: Distance from tractor's c.o.m. to rear axle.

c: Distance from tractor's rear axle to vertical joint.

ℓ_1: Distance from tractor's rear axle to front axle.

ℓ_2: Distance from trailer's axle to vertical joint.

Using this notation, by applying the Newton-Euler approach and imposing the appropriate holonomic and nonholonomic constraints, we obtain the following dynamic model of the vehicle (a detailed development of this model is given in Appendix A).

PROPOSITION 1. Under a slippage-free motion, the dynamics of the tractor-trailer robot are described by

$$\dot{v}_u = g_0 + \mathbf{g}_u \mathbf{F}_u + g_p f_p + g_s f_s \tag{1}$$

$$\dot{x} = \cos\theta_1 v_u \tag{2}$$

$$\dot{y} = \sin\theta_1 v_u \tag{3}$$

$$v_w = \frac{b v_u \tan\delta}{\ell_1} \tag{4}$$

$$\dot{\theta}_1 = \frac{v_u \tan\delta}{\ell_1} \tag{5}$$

$$\dot{\Phi} = -\frac{v_u}{\ell_1 \ell_2}\{\ell_1 \sin\Phi + (\ell_2 + c\cos\Phi)\tan\delta\} \tag{6}$$

$$\dot{\delta} = f_s, \tag{7}$$

where g_0, g_{u1}, g_{u2}, g_{u3}, g_p, and g_s are well-defined functions of x, y, θ_1, and Φ and of the vehicle's mass and geometric parameters (see Appendix A, eqs. (A26)–(A29)); $\mathbf{g}_u := [g_{u1} g_{u2} g_{u3}]$.

The vectors

$$\mathbf{q} := [x\ y\ \theta_1\ \Phi]', \tag{8}$$

$$\mathbf{v} := [v_u\ v_w\ \Omega_1\ \Omega_2]', \tag{9}$$

$$\mathbf{X} := [x\ y\ \theta_1\ \Phi\ v_u\ v_w\ \Omega_1\ \Omega_2]' := [\mathbf{q}'\ \mathbf{v}']' \tag{10}$$

and

$$\mathbf{a} := [a_u\ a_w\ a_{\theta 1}\ a_\Phi]', \tag{11}$$

are referred to as the *configuration* ($\mathbf{q}$), the *velocity* ($\mathbf{v}$), the *state* ($\mathbf{X}$), and the *acceleration* ($\mathbf{a}$) of the vehicle.

REMARK 1. By considering the mass parameters of the trailer to be equal to zero and by focusing attention on

Downloaded from ijr.sagepub.com at ARIZONA STATE UNIV on August 14, 2016

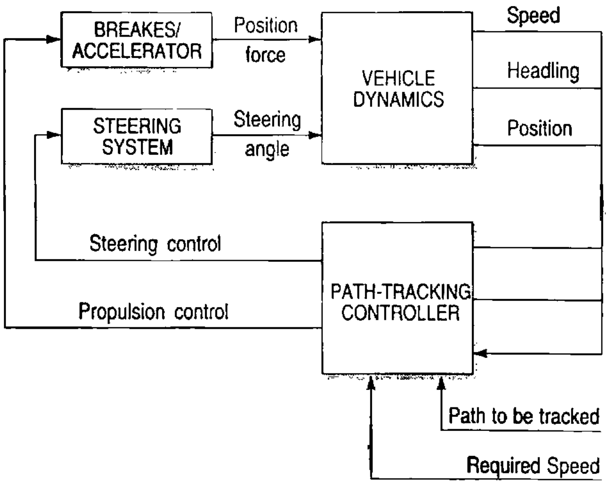

Fig. 3. Principle of operation of a path-tracking controller.

the dynamics of the tractor, eqs. (1)–(7) coincide with the model of a car-like robot given in DeSantis (1993).

3. Path Tracking

A path-tracking controller receives as input actual and desired values of the vehicle's speed, heading, and position relative to the path. It provides as output the propulsion and steering required to bring to zero the difference between actual and desired values (Fig. 3). In spite of its simplicity, a formal statement of this task requires a careful definition of the concepts of admissible path-tracking assignment, the vehicle's desired state, and path-tracking offsets. A *path-tracking assignment* is the combination of a path in the configuration space and a profile of the linear and angular velocities and accelerations with which this path is to be followed. A *path* (Latombe 1991) is described by a smooth vector function,

$$\mathbf{q}_p(s) := [x_p(s) y_p(s) \theta_{p1}(s) \Phi_p(s)]', \tag{12}$$

where $s\epsilon[0, \infty)$ is a parameter defining a point of the path, and $\mathbf{q}_p(s)$ represents the vehicle's required configuration at point s. *Velocity* and *acceleration profiles* along a path are described by a set of smooth functions

$$\mathbf{v}_p(s) := [v_{up}(s)\ v_{wp}(s)\ \Omega_{pi}(s)\ \Omega_{p2}(s)]', \tag{13}$$

$$\mathbf{a}_p(s) := [a_{up}(s)\ a_{wp}(s)\ a_{\theta p1}(s)\ a_{\Phi p2}(s)]',\ s\epsilon[0, \infty), \tag{14}$$

where $\mathbf{v}_p(s)$ and $\mathbf{a}_p(s)$ are the velocity and the acceleration that the vehicle should have when its workspace position corresponds to $(x_p(s), y_p(s))$. A path-tracking assignment is *admissible* if eqs. (13) and (14) are compatible with eqs. (2)–(7).

Given a state of the vehicle $\mathbf{X} := [x\ y\ \theta_1\ \Phi\ v_u\ v_w\ \Omega_1\ \Omega_2]'$, the vehicle's *desired state* corresponding to an admissible path-tracking assignment is defined by

$$\mathbf{x}_d := [\mathbf{q}_d'\ \mathbf{v}_d']', \tag{15}$$

$$\mathbf{q}_d := [x_d\ y_d\ \theta_{d1}\ \Phi_d]' \tag{16}$$

$$\mathbf{v}_d := [v_{ud}\ v_{wd}\ \Omega_{d1}\ \Omega_{d2}]', \tag{17}$$

with

$$[x_d\ y_d\ \theta_{d1}\ \Phi_d] := [x_p(\sigma)\ y_p(\sigma)\ \theta_{p1}(\sigma)\ \Phi_p(\sigma)], \tag{18}$$

and

$$[v_{ud}\ v_{wd}\ \Omega_{d2}\ \Omega_{d2}] := [v_{up}(\sigma)\ v_{wp}(\sigma)\ \Omega_{p1}(\sigma)\ \Omega_p(\sigma)], \tag{19}$$

where $\sigma\epsilon[0, \infty)$ has the property that $(x_p(\sigma), y_p(\sigma))$ is the point of the workspace path closest (in Euclidean norm) to (x, y).

The *path-tracking offsets* (*velocity* (v_{os}), *heading* (θ_{os}, Φ_{os}), *lateral* (l_{os}), and *steering* (δ_{os}) offsets) are defined by

$$v_{os}(t) := v_u(t) - v_{ud}(t) \tag{20}$$

$$\theta_{os}(t) := \theta_1(t) - \theta_{d1}(t) \tag{21}$$

$$\Phi_{os}(t) := \Phi(t) - \Phi_d(t) \tag{22}$$

$$\ell_{os}(t) := -\{x(t) - x_d(t)\} \sin\theta_{d1}(t) + \{y(t) - y_d(t)\} \cos\theta_{d1}(t) \tag{23}$$

$$\delta_{os}(t) := \delta(t) - \delta_d(t). \tag{24}$$

where

$$\delta_d := \tan^{-1} \frac{\Omega_{d1} l_1}{v_{ud}}. \tag{25}$$

It should be noted that while the meanings of v_{os}, θ_{os}, Φ_{os}, and δ_{os} are rather obvious the lateral offset, ℓ_{os}, represents the (signed) distance between the guide point of the vehicle and the assigned path in the workspace (Fig. 4).

The task of a *path-tracking* controller may now be formally stated as that of generating the propulsion and steering controls required to have

$$\lim_{t\to\infty.} [v_{os}(t)\ \theta_{os}(t)\ \Phi_{os}(t)\ \ell_{os}(t)] = 0. \tag{26}$$

REMARK 2. The above statement gives a precise mathematical formulation of the intuitive notion of geometric path tracking that is currently used in actual implementations of car-like robots. By simply replacing Φ_{os} with $\Phi_{osi}, i = 1, 2, \ldots$, where Φ_{osi} would denote the heading offset of the ith trailer, this statement becomes applicable to tractors with multiple trailers.

REMARK 3. Our notions of desired state and geometric path tracking rely on the assumption that the projection

Downloaded from ijr.sagepub.com at ARIZONA STATE UNIV on August 14, 2016

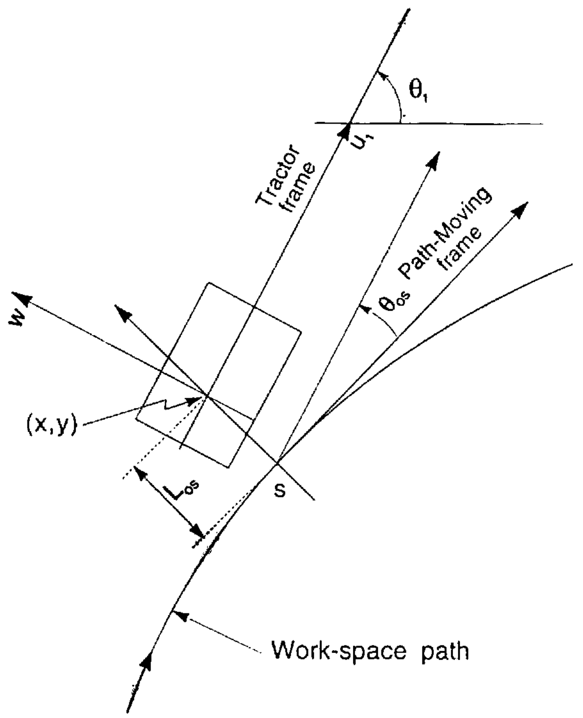

Fig. 4. Lateral and tractor's heading offsets.

of a vehicle state onto the planar xy path is well defined and that a unique state from the path-tracking assignment can be associated with it. While these assumptions are satisfied in many practical applications, this is not usually true in the general case. It follows that it is important to clarify under what conditions these assumptions do indeed hold and to develop appropriate techniques to deal with the cases where they do not hold. Questions about the continuity of the projection and the complexity associated with its computation also represent important topics of investigation. In spite of their importance, these issues fall beyond the boundary of the present article, and the reader is referred to the specialized literature (Schwartz and Yap 1987; Latombe 1991).

4. Controller Design

With the above background, the design of a path-tracking controller may be viewed as equivalent to the following stabilization problem.

PROPOSITION 2. Under a slippage-free motion, path tracking is equivalent to stabilizing the dynamic system.

$$\dot{v}_{os} = u_1(t) \tag{27}$$

$$\dot{\theta}_{os} = \frac{(v_{ud} + v_{os})}{\ell_1}(\tan(\delta_d + \delta_{os}) - \tan\delta_d) \tag{28}$$

$$\begin{aligned}\dot{\Phi}_{os} = \frac{(v_{ud} + v_{os})}{\ell_1 \ell_2}\{&\ell_1(\sin\Phi_d - \sin(\Phi_d + \Phi_{os})) \\ &+ (\ell_2 + c\cos\Phi_d)\tan\delta_d \\ &- (\ell_2 + c\cos(\Phi_d + \Phi_{os}))\tan(\delta_d + \delta_{os})\}\end{aligned} \tag{29}$$

$$\dot{\ell}_{os} = (v_{ud} + v_{os})\sin\theta_{os} \tag{30}$$

$$\dot{\delta}_{os} = u_2(t), \tag{31}$$

where

$$u_1 := -\dot{v}_{ud} + g_0 + \mathbf{g}_u\mathbf{F}_u + g_p f_p + g_s f_s, \tag{32}$$

$$u_2 := -\dot{\delta}_d + f_s. \tag{33}$$

With this result, a path-tracking controller may now be designed by bringing to bear well-known control theory techniques.

PROPOSITION 3. Under a slippage-free motion and with small offsets, path tracking is equivalent to stabilizing the linear system

$$\dot{\mathbf{x}} = \mathbf{A}\mathbf{x} + \mathbf{B}\mathbf{u}, \tag{34}$$

where

$$\mathbf{x} := [v_{os}\ \theta_{os}(t)\ \Phi_{os}(t)\ \ell_{os}(t)\ \delta_{os}(t)]' \tag{35}$$

$$\mathbf{B} := \begin{bmatrix} 1 & 0 & 0 & 0 & 0 \\ 0 & 0 & 0 & 0 & 1 \end{bmatrix}' \tag{36}$$

and

$$\mathbf{A} := \begin{bmatrix} 0 & 0 & 0 & 0 & 0 \\ 0 & 0 & 0 & 0 & \frac{v_{ud}}{\ell_1\cos^2\delta_d} \\ 0 & 0 & a_{33} & 0 & a_{35} \\ 0 & v_{ud} & 0 & 0 & 0 \\ 0 & 0 & 0 & 0 & 0 \end{bmatrix} \tag{37}$$

with

$$a_{33} := -v_{ud}\left\{\frac{\cos\Phi_d}{\ell_2} - \frac{c\tan\delta_d\sin\Phi_d}{\ell_1\ell_2}\right\} \tag{38}$$

and

$$a_{35} := -v_{ud}\frac{\ell_2 + c\cos\Phi_d}{\ell_2\ell_1\cos^2\delta_d}. \tag{39}$$

PROPOSITION 4. If the path in the workspace is a straight line or a circular arc, the tracking velocity is constant, and the path-tracking offsets are kept sufficiently small, then path-tracking may be ensured by combining two linear and time-invariant controllers; first, a steering controller providing the steering action

$$f_s(t) = -\mathbf{K}_s[\theta_{os}(t)\ \Phi_{os}(t)\ \ell_{os}(t)\ \delta_{os}(t)], \tag{40}$$

where $\mathbf{K}_s$ is a row-vector of constant gains; second, a speed controller providing the propulsion

$$f_p(t) = f_{p1}(t) + f_{p2}(t), \tag{41}$$

where

$$f_{p1} = g_p^{-1}\{\dot{v}_{ud} - g_0 - \mathbf{g}_u\mathbf{F}_u - g_s f_s\} \tag{42}$$

Downloaded from ijr.sagepub.com at ARIZONA STATE UNIV on August 14, 2016

with f_s given by eq. (40) and

$$f_{p2} = -g_p^{-1}\{k_{p1}v_{os} + k_{p2}\int v_{os}\,dt\}, \tag{43}$$

with k_{p1} and k_{p2} constant gains.

PROPOSITION 5. The controller described by Proposition 4 has the following properties:

(a) the dynamics of v_{os} are described by .

$$\ddot{v}_{os} - (p_{11} + p_{12})\dot{v}_{os} + p_{11}p_{12}v_{os} = 0, \tag{44}$$

where

$$k_{p1} = -(p_{11} + p_{12}), \quad k_{p2} = p_{11}p_{12}, \tag{45}$$

and p_{11}, p_{12} are the eigenvalues of eq. (44).

(b) gains $\mathbf{K}_s := [k_{s1}\ k_{s2}\ k_{s3}\ k_{s4}]$ may be chosen so as to stabilize

$$\dot{\mathbf{x}} = \mathbf{A}\mathbf{x} + \mathbf{B}\mathbf{u},$$
$$\mathbf{u} = -\mathbf{K}_s\mathbf{x}, \tag{46}$$

where

$$\mathbf{B} := [0\ 0\ 0\ 1]' \tag{47}$$

and

$$\mathbf{A} := \begin{bmatrix} 0 & 0 & 0 & \frac{v_{ud}}{\ell_1 \cos^2 \delta_d} \\ 0 & a_{22} & 0 & a_{24} \\ v_{ud} & 0 & 0 & 0 \\ 0 & 0 & 0 & 0 \end{bmatrix} \tag{48}$$

with

$$a_{22} := v_{ud}\left\{\frac{\cos\Phi_d}{\ell_2} - \frac{c\tan\delta_d \sin\Phi_d}{\ell_1\ell_2}\right\} \tag{49}$$

and

$$a_{24} := -v_{ud}\frac{(\ell_2 + c\cos\Phi_d)}{\ell_1\ell_2\cos^2\delta_d}. \tag{50}$$

PROPOSITION 6. The steering controller described by eq. (40) may be replaced with

$$f_s(t) = -\mathbf{K}_s[\ell_{os}(t)\ \dot{\ell}_{os}(t)\ \Phi_{os}(t)\ \delta_{os}(t)]', \tag{51}$$

where $\mathbf{K}_s$ is a row vector of constant gains. In the case of a forward motion, ($v_{ud} > 0$), a suitable steering controller is given by

$$f_s(t) = -\mathbf{K}_s[\ell_{os}(t)\ \dot{\ell}_{os}(t)\ \delta_{os}(t)]', \tag{52}$$

where, once again, $\mathbf{K}_s$ is a row vector of constant gains.

REMARK 4. By considering the mass parameters of the trailer to be equal to zero and by focusing attention on the dynamics of the tractor, Propositions 2 through 6 enable a rediscovery and an extension of results relevant to path-tracking controllers for car-like robots. This extension means that the procedures currently available for designing these controllers now become applicable to more general paths, as well as to the case where the tracking velocity is no longer constrained to be constant (DeSantis 1993; 1994b).

REMARK 5. The structure of eqs. (27)–(33) and (34)–(39) reveals that, under the hypothesis of a slippage-free motion, the influence of external perturbations (incorporated in our model in the vector $\mathbf{F}_u$) and mass parameter variations over the vehicle's dynamics satisfies the so-called matching conditions (Corless 1993). It follows that the stabilization problem considered in Proposition 2 may be given a solution that is robust with respect to this influence; the performance of the controllers in Propositions 3 through 6 could be made robust by equipping these controllers with the addition of an appropriate feedback loop (DeSantis 1994a). On the other hand, it should be noted that the influence produced by variations of the geometric parameters (c, ℓ_1, and ℓ_2) does not satisfy the matching conditions. As a consequence, the various controllers that we have considered cannot be made robust with respect to such an influence.

5. An Application Example

Consider the design of a path-tracking controller for a tractor-trailer–like robot characterized by the following geometric parameters:

$$c = 1m, \quad \ell_1 = 2m, \quad \text{and} \quad \ell_2 = 4m. \tag{53}$$

Let the path-tracking assignment require this vehicle to follow a circular path of radius $r = 20\,\mathrm{m}$, with a velocity equal to 2.5 m/s. By following the procedure suggested by Propositions 4 and 5, path-tracking may be ensured by means of a controller made up of a steering component and a speed component.

The steering controller is described by

$$f_s(t) = -\mathbf{K}_s[\theta_{os}(t)\ \Phi_{os}(t)\ \ell_{os}(t)\ \delta_{os}(t)], \tag{54}$$

where gain row vector $\mathbf{K}_s$ is chosen so as to stabilize $\mathbf{A} - \mathbf{B}\mathbf{K}_s$, with matrices $\mathbf{A}$ and $\mathbf{B}$ as in eqs. (36) and (37). The values of δ_d and Φ_d, on which matrix $\mathbf{A}$ depends, are computed using eqs. (5) and (6). These equations imply

$$\delta_d = \tan^{-1}\left(\frac{\Omega_{1d}\ell_1}{v_{ud}}\right) = \tan^{-1}\left(\frac{\ell_1}{r}\right) \tag{55}$$

and

$$r\sin\Phi_d + c\cos\Phi_d = -\ell_2. \tag{56}$$

With the assigned values of c, ℓ_1, ℓ_2, and r, it follows that $\delta_d = 0.1$ and $\Phi_d = -0.251$. Corresponding to a forward motion ($v_{ud} = 2.5$: the tractor pulls the trailer), we then have

$$\mathbf{A} := \begin{bmatrix} 0 & 0 & 0 & 1.2 \\ 0 & -.73 & 0 & -1.57 \\ 2.5 & 0 & 0 & 0 \\ 0 & 0 & 0 & 0 \end{bmatrix}. \tag{57}$$

Downloaded from ijr.sagepub.com at ARIZONA STATE UNIV on August 14, 2016

and, corresponding to a backward motion ($v_{ud} = -2.5$: the tractor pushes the trailer),

$$\mathbf{A} := \begin{bmatrix} 0 & 0 & 0 & -1.2 \\ 0 & .73 & 0 & 1.57 \\ -2.5 & 0 & 0 & 0 \\ 0 & 0 & 0 & 0 \end{bmatrix}. \tag{58}$$

By computing $\mathbf{K}_s$ via the linear quadratic optimization (LQR) approach, we have $\mathbf{K}_s = \mathbf{S}^{-1}\,\mathbf{B}'\mathbf{P}$, where $\mathbf{P}$ is the solution of the Riccati equation (Chen 1987)

$$\mathbf{A}'\mathbf{P} - \mathbf{P}\mathbf{B}\mathbf{S}^{-1}\mathbf{B}' + \mathbf{P}\mathbf{A} + \mathbf{Q} = 0, \tag{59}$$

and $\mathbf{Q}$ and $\mathbf{S}$ are conveniently selected positive definite matrices. Note that an appropriate selection depends on whether a forward or a backward motion is considered and is usually more laborious in the case of a backward motion. For a forward motion, with the selection $\mathbf{S} = .1\mathbf{I}_4$ and $\mathbf{Q} = \mathbf{I}_4$, we obtain

$$k_{s1} = 6.9 \quad k_{s2} = -.25 \quad k_{s3} = 3.16 \quad k_{s4} = 6. \tag{60}$$

For a backward motion, with $\mathbf{S} = \mathbf{I}_4$ and $\mathbf{Q} = \mathrm{diag}[q_i]$, and with $q_1 = q_2 = 0.1$, $q_3 = 100$, and $q_4 = 10$, we obtain

$$k_{s1} = 98.8 \quad k_{s2} = 95.7 \quad k_{s3} = -10.0 \quad k_{s4} = 9.2. \tag{61}$$

The speed controller generates a propulsion given by

$$f_p = g_p^{-1}\{-g_0 - \mathbf{g}_u\hat{\mathbf{F}}_u - g_s f_s\} - g_p^{-1}\{k_{p1}v_{os} + k_{p2}\int v_{os}\,dt\}, \tag{62}$$

where $\hat{\mathbf{F}}_u$ denotes the estimated effect of longitudinal perturbation forces acting on the tires, f_s is as in eq. (54), and g_0, $\mathbf{g}_u$, g_s, and g_p are as in Proposition 1. By requiring the dynamics of the velocity offset to be characterized by the poles $p_{11} = -6$ and $p_{12} = -0.1$ and applying eq. (45), we obtain $k_{p1} = 6.1$ and $k_{p2} = .6$.

Figures 5 and 6 show typical (simulated) vehicle responses corresponding to a forward motion under nominal operating conditions (that is, actual values of the vehicle's kinematic and mass parameters equal to expected values and absence of external perturbations). Figures 7 and 8 show typical responses obtained under the same conditions for a backward motion. In accordance with everyday experience, note that in the backward motion the region of attraction in the offset space is smaller than in forward motion. Moreover, in the backward motion the offsets have a more pronounced transient dynamics. In spite of this fact, the performance of the controller appears to be satisfactory in both forward and backward motion, and this under initial path-tracking offsets of the size that we would expect to find in the transitions associated with the tracking of more realistic paths made of several linear or circular segments.

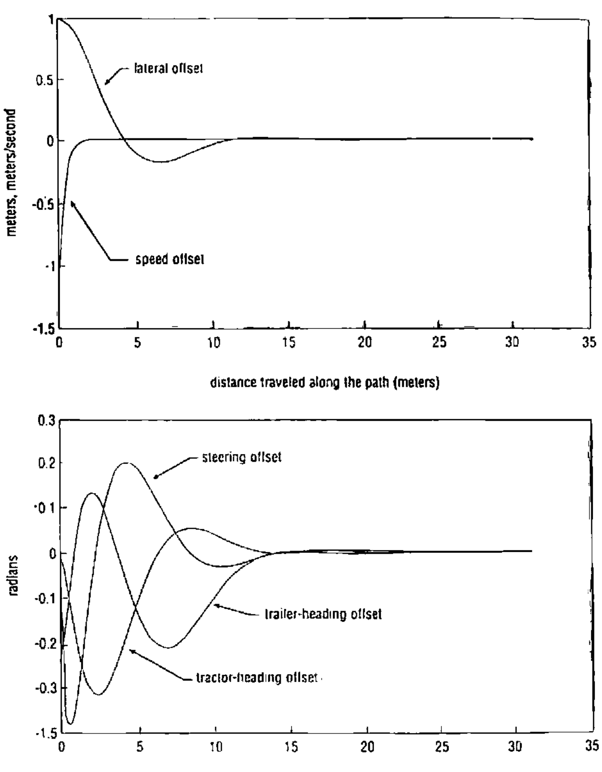

Fig. 5. Forward circular maneuver: path-tracking offsets.

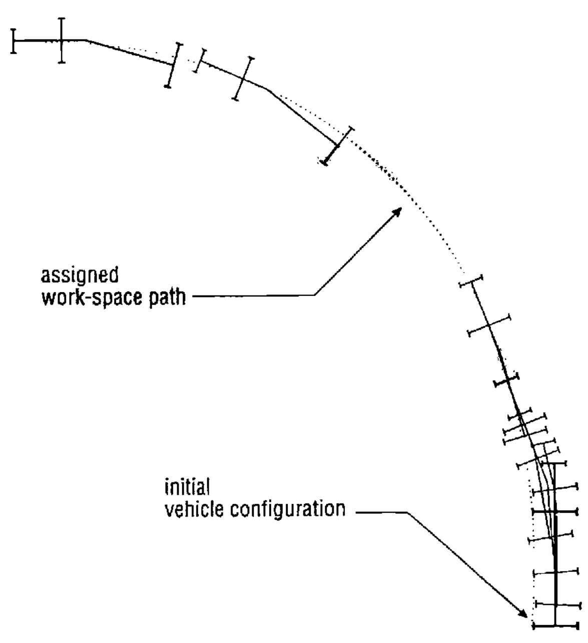

Fig. 6. Forward circular maneuver: vehicle's motion in workspace.

Downloaded from ijr.sagepub.com at ARIZONA STATE UNIV on August 14, 2016

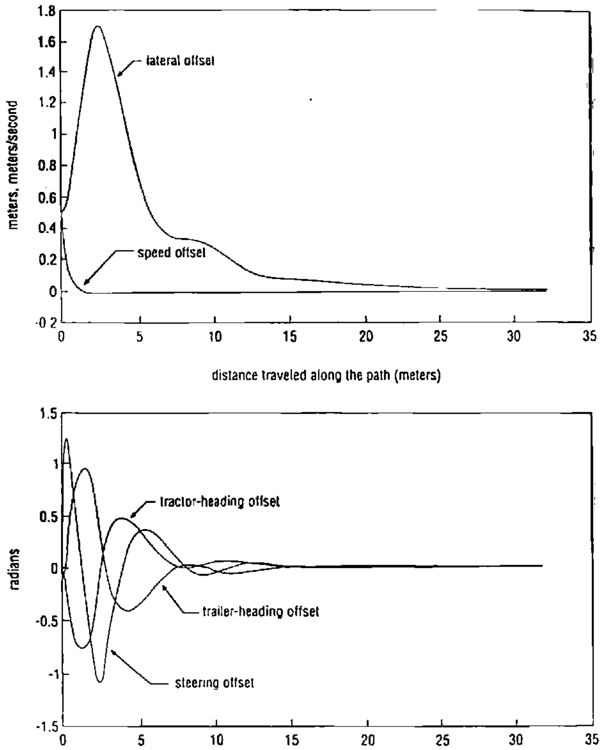

Fig. 7. Backward circular maneuver: path-tracking offsets.

The behavior of the vehicle was also simulated under more general operating conditions characterized by such factors as the presence of external perturbations (longitudinal and lateral drag), an incorrect estimate of the vehicle's parameters (mass and geometric parameters and parameters of the radius of the circular path), and more realistic representations of the forces of contact between the tires and the surface of motion. (More details on simulation modalities are given in Appendix B.) The ensuing results have shown the controller's performance to be reasonably robust with respect to all these factors, not only when the hypothesis of a slippage-free motion is satisfied (as predicted in part by Remark 5), but also under a relaxation of this hypothesis. On the other hand, experimental evidence has shown that in this type of study the correspondence between simulation and experimental results is generally quite good (Borenstein and Koren 1987; DeSantis and Hurteau 1990). It is therefore reasonable to anticipate that no major difficulty should be encountered in a practical implementation of the proposed controller.

Conclusions

By assuming a slippage-free motion, it is possible to considerably simplify the model of the kinematic and

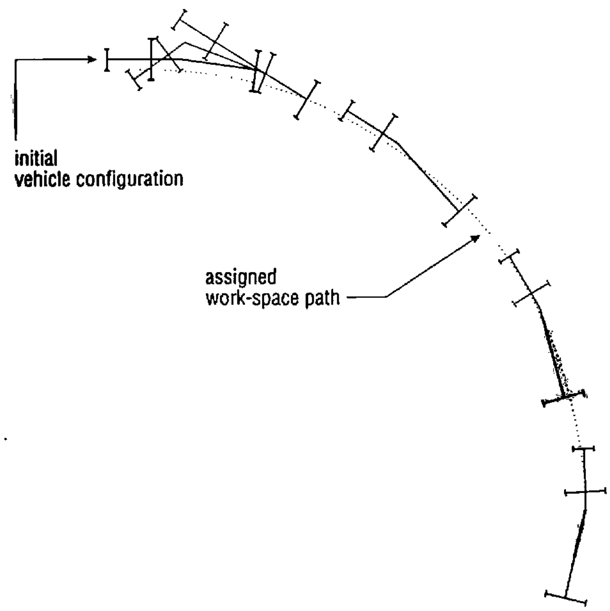

Fig. 8. Backward circular maneuver: vehicle's motion in workspace.

dynamic behavior of a tractor-trailer–like robot (Proposition 1). Combined with a geometric notion of path-tracking, this simplification leads, in turn, to a simplified description of the dynamics of lateral, heading, and velocity path-tracking offsets (Proposition 2). It follows that, for small offsets, path-tracking may be ensured by means of an affine controller, linear with respect to these offsets (Proposition 3). Corresponding to straight-line or circular paths to be followed with a constant velocity, this controller may be implemented by means of a steering component generating steering as a function of lateral and heading offsets, and of a speed component providing propulsion as a function of steering action and speed offset (Proposition 4). The design of these components may be carried out by using proportional-integral-derivative (PID) and state-feedback time-invariant techniques (Proposition 5). Simplified versions of the steering controller, in which the tractor's heading offset may be replaced by a measurement of the rate of lateral offset, are also available (Proposition 6). Finally, by removing from our equations the influence of the trailer, we rediscover and generalize results available for car-like robots (DeSantis 1993; 1994b).

Prospects for a successful practical implementation of the proposed controller appear to be quite promising. Preliminary simulations suggest the controller's performance to be reasonably robust not only with respect to path-tracking offsets, external perturbations, and parameter variations, but also with respect to a relaxation of the hypothesis of a slippage-free motion on which the controller

Downloaded from ijr.sagepub.com at ARIZONA STATE UNIV on August 14, 2016

design is based. Technological requirements are similar to those currently encountered in the robotization of more conventional vehicles and should be adequately met by means of standard components such as optical encoders, accelerometers, gyros, CCD cameras, laser range finders, sonars, and other similar components. On the other hand, it should be noted that more theoretical and experimental work is required before the full potential of the proposed controller can be conveniently assessed. For example, one particular area in which further theoretical research is needed concerns the investigation of questions such as well-posedness, continuity, and computational complexity of the notion of geometric path-tracking. These questions remain open in the context of paths more general than the linear and circular paths on which we have focused attention.

Appendix A: More on the Dynamics of the Vehicle

In addition to the notation introduced in Section 2, we denote with m_1 and m_2 the mass of the tractor and trailer; with j_1, j_2 the yaw moments of inertia about their centers of mass; and with f_{w1}, f_{w2}, and f_{w3} the lateral forces exerted by the tires on the vehicle. The application of the Newton-Euler approach leads to the following vehicle dynamics (Ellis 1969; Kane and Levinson 1985; Saha and Angeles 1989)

$$\dot{x} = v_u \cos\theta_1 - (v_w - b * \Omega_1)\sin\theta_1 \tag{A1}$$
$$\dot{y} = v_u \sin\theta_1 + (v_w - b * \Omega_1)\cos\theta_1 \tag{A2}$$
$$\dot{\theta}_1 = \Omega_1 \tag{A3}$$
$$\dot{\theta}_2 = \Omega_2 \tag{A4}$$
$$\dot{\mathbf{v}} = \mathbf{D}^{-1}\{\mathbf{G}_0 + \mathbf{G}_w\mathbf{F}_w + \mathbf{G}_u\mathbf{F}_u + \mathbf{G}_p f_p\} \tag{A5}$$

where

$$\mathbf{v} := [v_u\ v_w\ \Omega_1\ \Omega_2]' \tag{A6}$$
$$\mathbf{F}_w := [f_{w1}\ f_{w2}\ f_{w3}]' \tag{A7}$$
$$\mathbf{F}_u := [f_{u1}\ f_{u2}\ f_{u3}]' \tag{A8}$$

and

$$\mathbf{D} := \begin{bmatrix} m_1 + m_2 & 0 & 0 & m_2 e\sin\Phi \\ 0 & m_1 + m_2 & -m_2(c+b) & -m_1 e\cos\Phi \\ 0 & -m_2(c+b) & j_1 + m_2(c+b)^2 & m_2 e(c+b)\cos\Phi \\ m_2 e\sin\Phi & -m_2 e\cos\Phi & m_2 e(c+b)\cos\Phi & j_2 + m_2 e^2 \end{bmatrix} \tag{A9}$$

$$\mathbf{G}_0 := \begin{bmatrix} (m_1+m_2)v_w\Omega_1 - m_2 d\Omega_1^2 - em_2\Omega_2^2\cos\Phi \\ -(m_1+m_2)v_u\Omega_1 - em_2\Omega_2^2\sin\Phi \\ m_2 v_u\Omega_1(c+b) + m_2 d(c+b)\Omega_2^2\sin\Phi \\ m_2 e(v_u\cos\Phi + v_w\sin\Phi)\Omega_1 \end{bmatrix} \tag{A10}$$

$$\mathbf{G}_w := \begin{bmatrix} \sin\delta & 0 & -\sin\Phi \\ \cos\delta & 1 & \cos\Phi \\ a\cos\delta & -b & (c+b)\cos\Phi \\ 0 & 0 & -(d+e) \end{bmatrix} \tag{A11}$$

$$\mathbf{G}_u := \begin{bmatrix} \cos\delta & 1 & \cos\Phi \\ \sin\delta & 0 & \sin\Phi \\ a\sin\delta & 0 & (c+b)\sin\Phi \\ 0 & 0 & 0 \end{bmatrix} \tag{A12}$$

$$\mathbf{G}_p := [1\ 0\ 0\ 0]' \tag{A13}$$
$$\Phi := \theta_2 - \theta_1. \tag{A14}$$
$$\dot{\delta} = f_s. \tag{A15}$$

By imposing that the motion of the vehicle be slippage-free, we obtain the following lemmas.

Lemma 1. Under a slippage-free motion, the lateral forces exerted by the tires on the tractor-trailer robot are given by

$$\mathbf{F}_w = \mathbf{G}_1 + \mathbf{G}_2\mathbf{F}_u + \mathbf{G}_3 f_p + \mathbf{G}_4 f_s, \tag{A16}$$

where

$$\mathbf{G}_1 := \mathbf{T}\mathbf{G}_0 + [\mathbf{H}\mathbf{D}^{-1}\mathbf{G}_w]^{-1}\mathbf{H}_0 \tag{A17}$$
$$\mathbf{G}_2 := \mathbf{T}\mathbf{G}_u \tag{A18}$$
$$\mathbf{G}_3 := \mathbf{T}\mathbf{G}_p \tag{A19}$$
$$\mathbf{G}_4 := [\mathbf{H}\mathbf{D}^{-1}\mathbf{G}_w]^{-1}\mathbf{G}_s \tag{A20}$$
$$\mathbf{T} := -[\mathbf{H}\mathbf{D}^{-1}\mathbf{G}_w]^{-1}\mathbf{H}\mathbf{D}^{-1} \tag{A21}$$

$$\mathbf{H} := \begin{bmatrix} -\frac{b\tan\delta}{\ell_1} & 1 & 0 & 0 \\ -\frac{\tan\delta}{\ell_1} & 0 & 1 & 0 \\ h_{13} & 0 & 0 & 1 \end{bmatrix} \tag{A22}$$

with

$$h_{13} := \frac{\sin\Phi}{\ell_2} + \frac{c\cos\Phi\tan\delta}{\ell_1\ell_2} \tag{A23}$$
$$\ell_1 := a + b, \quad \ell_2 := d + e, \tag{A24}$$

and

$$\mathbf{G}_s := \left[\frac{bv_u}{\ell_1\cos^2\delta} \quad \frac{v_u}{\ell_1\cos^2\delta} \quad -\frac{cv_u\cos\Phi}{\ell_1\ell_2\cos^2\delta}\right]'. \tag{A25}$$

$$\mathbf{H}_0 := \left[0 \mid 0 \mid \frac{-(\Omega_2 - \Omega_1)v_u\cos\Phi}{\ell_2} + \frac{c(\Omega_2 - \Omega_1)v_u\tan\delta\sin\Phi}{\ell_1\ell_2}\right]' \tag{A26}$$

with $\mathbf{G}_0$, $\mathbf{G}_w$, $\mathbf{G}_u$, $\mathbf{G}_p$ as in eqs. (A10)–(A13).

Downloaded from ijr.sagepub.com at ARIZONA STATE UNIV on August 14, 2016

LEMMA 2. The functions g_0, $\mathbf{g}_u$, g_p, and g_s that describe the motion of the vehicle under a slippage-free motion (see Proposition 1) are computed as follows:

$$g_0 := [1\ 0\ 0\ 0]\mathbf{D}^{-1}\{\mathbf{G}_0 + \mathbf{G}_w\mathbf{G}_1\} \tag{A27}$$
$$\mathbf{g}_u := [1\ 0\ 0\ 0]\mathbf{D}^{-1}\{\mathbf{G}_u + \mathbf{G}_w\mathbf{G}_2\} \tag{A28}$$
$$g_p := [1\ 0\ 0\ 0]\mathbf{D}^{-1}\{\mathbf{G}_p + \mathbf{G}_w\mathbf{G}_3\} \tag{A29}$$
$$g_s := [1\ 0\ 0\ 0]\mathbf{D}^{-1}\mathbf{G}_w\mathbf{G}_4 \tag{A30}$$

with $\mathbf{G}_1$, $\mathbf{G}_2$, $\mathbf{G}_3$, $\mathbf{G}_4$ as in eqs. (A17)–(A26), and $\mathbf{G}_0$, $\mathbf{G}_u$, $\mathbf{G}_p$, $\mathbf{G}_w$ as in eqs. (A10)–(A13).

Proof (Lemma 1): In a slippage-free motion, longitudinal, lateral, and angular velocities of a mobile wheeled vehicle are interdependent. For the tractor-trailer under study, a direct inspection reveals this interdependence to be described by

$$\Omega_1 = \frac{v_u}{\ell_1}\tan\delta, \tag{A31}$$
$$v_w = b\Omega_1 = \frac{bv_u\tan\delta}{\ell_1}, \tag{A32}$$
$$\Omega_2 = -\frac{v_u}{\ell_2}\sin\Phi - \frac{cv_u\cos\Phi\tan\delta}{\ell_1\ell_2}, \tag{A33}$$
$$\dot{\Phi} = \Omega_2 - \Omega_1 \tag{A34}$$
$$= -\frac{v_u}{\ell_1\ell_2}\{\ell_1\sin\Phi + (\ell_2 + c\cos\Phi)\tan\delta\}.$$

These equations imply

$$\mathbf{H}\mathbf{v} = 0, \tag{A35}$$

where $\mathbf{v} := [v_u\ v_w\ \Omega_1\ \Omega_2]'$, and

$$\mathbf{H} := \begin{bmatrix} -\frac{b\tan\delta}{\ell_1} & 1 & 0 & 0 \\ -\frac{\tan\delta}{\ell_1} & 0 & 1 & 0 \\ h_{13} & 0 & 0 & 1 \end{bmatrix} \tag{A36}$$

with

$$h_{13} := \frac{\sin\Phi}{\ell_2} + \frac{c\cos\Phi\tan\delta}{\ell_1\ell_2}. \tag{A37}$$

Now premultiply both members of eq. (A5) by $\mathbf{H}$ to obtain

$$\mathbf{H}\dot{\mathbf{v}} = \mathbf{H}\mathbf{D}^{-1}\{\mathbf{G}_0 + \mathbf{G}_w\mathbf{F}_w + \mathbf{G}_u\mathbf{F}_u + \mathbf{G}_p f_p\}, \tag{A38}$$

and differentiate eq. (A35) to obtain

$$\mathbf{H}\dot{\mathbf{v}} = -\dot{\mathbf{H}}\mathbf{v}, \tag{A39}$$

where

$$\dot{\mathbf{H}} = \begin{bmatrix} -\frac{bF_s}{\ell_1\cos^2\delta} & 0 & 0 & 0 \\ -\frac{f_s}{\ell_1\cos^2\delta} & 0 & 0 & 0 \\ \dot{h}_{13} & 0 & 0 & 0 \end{bmatrix} \tag{A40}$$

with

$$\dot{h}_{13} = \frac{\ell_1\cos\Phi - c\tan\delta\sin\Phi}{\ell_1\ell_2}\dot{\Phi} + \frac{c\cos\Phi}{\ell_1\ell_2\cos^2\delta}f_s. \tag{A41}$$

From eqs. (A39) and (A40) it follows that

$$\mathbf{H}\dot{\mathbf{v}} = \mathbf{G}_s f_s + \mathbf{H}_0, \tag{A42}$$

with

$$\mathbf{G}_s := \left[\frac{bv_u}{\ell_1\cos^2\delta}\quad \frac{v_u}{\ell_1\cos^2\delta}\quad -\frac{c\cos\Phi v_u}{\ell_1\ell_2\cos^2\delta}\right]' \tag{A43}$$

and

$$\mathbf{H}_0 := \left[0 \mid 0 \mid \frac{-\cos\Phi(\Omega_2 - \Omega_1)v_u}{\ell_2} + \frac{c\tan\delta\sin\Phi(\Omega_2 - \Omega_1)v_u}{\ell_1\ell_2}\right]'. \tag{A44}$$

By combining eqs. (A38) with (A42), we have

$$\mathbf{H}\mathbf{D}^{-1}\mathbf{G}_w\mathbf{F}_w = -\mathbf{H}\mathbf{D}^{-1}\{\mathbf{G}_0 + \mathbf{G}_u\mathbf{F}_u + \mathbf{G}_p f_p\} - \mathbf{G}_s f_s + \mathbf{H}_0 \tag{A45}$$

and therefore eqs. (A17)–(A26). □

Proof (Lemma 2): From eqs. (A5) and (A6), we have

$$\dot{v}_u = [1\ 0\ 0\ 0]\mathbf{D}^{-1}\{\mathbf{G}_0 + \mathbf{G}_w\mathbf{F}_w + \mathbf{G}_u\mathbf{F}_u + \mathbf{G}_p f_p\} \tag{A46}$$

and, by replacing $\mathbf{F}_w$ with eq. (A16),

$$\dot{v}_u = [1\ 0\ 0\ 0]\mathbf{D}^{-1}\{\mathbf{G}_0 + \mathbf{G}_u\mathbf{F}_u + \mathbf{G}_p f_p + \mathbf{G}_w\mathbf{G}_1 + \mathbf{G}_w\mathbf{G}_2\mathbf{F}_u + \mathbf{G}_w\mathbf{G}_3 f_p + \mathbf{G}_w\mathbf{G}_4 f_s\}. \tag{A47}$$

It follows that

$$\dot{v}_u = [1\ 0\ 0\ 0]\mathbf{D}^{-1}\{\mathbf{G}_0 + \mathbf{G}_w\mathbf{G}_1 + (\mathbf{G}_u + \mathbf{G}_w\mathbf{G}_2)\mathbf{F}_u + (\mathbf{G}_p + \mathbf{G}_w\mathbf{G}_3)f_p + \mathbf{G}_w\mathbf{G}_4 f_s\}, \tag{A48}$$

hence eqs. (A27)–(A30). □

Appendix B: Simulation of the Path-tracking Controller

While the path-tracking controller is designed by assuming slippage-free motion—and therefore by using eqs. (A1)–(A7)—simulations of its performance were carried out by considering the more general vehicle model described by eqs. (A1)–(A15). In applying this model the lateral forces exerted by the tires on the vehicle were represented as a function of the *sideslip angles* (i.e., the angle between the tire's longitudinal axis and the velocity

Downloaded from ijr.sagepub.com at ARIZONA STATE UNIV on August 14, 2016

of the tire's point of contact with the surface of motion). In particular, we adopted the linear representation

$$f_{w1} := -c_1\beta_1 \tag{B1}$$

$$f_{w2} := -c_2\beta_2 \tag{B2}$$

$$f_{w3} := -c_3\beta_3 \tag{B3}$$

where c_1, c_2, and c_3 are stiffness factors, and β_i is the sideslip angle. (Such a representation has been used by, among others, Ellis 1969, Matsumoto and Tomizuka 1992, and Hemami et al. 1992). Following common practice, the sideslip angles were computed as a function of the steering angle and of the vehicle's lateral, longitudinal, and angular velocities. In the case of a forward motion, we have, for example

$$\beta_1 = \tan^{-1}\left\{\frac{v_w + a\Omega_1}{v_u}\right\} - \delta \tag{B4}$$

$$\beta_2 = \tan^{-1}\left\{\frac{v_w - b\Omega_1}{v_u}\right\} \tag{B5}$$

and

$$\beta_3 = \tan^{-1}\left\{\frac{v_u \sin\Phi + (v_w - d\Omega_1)\cos\Phi - \ell_2\Omega_2}{v_u\cos\Phi - (v_w - d\Omega_1)\sin\Phi}\right\}. \tag{B6}$$

In addition to the geometric parameters specified in the controller's design, the following vehicle mass and stiffness parameters were used: $a = b = 1\,\mathrm{m}$, $d = 2\,\mathrm{m}$, $m_1 = 400\,\mathrm{kg}$, $m_2 = 600\,\mathrm{kg}$, $j_1 = 200\,\mathrm{Kg^*m^2}$, $j_2 = 400\,\mathrm{Kg^*m^2}$, and $c_1 = c_2 = c_3 = 60{,}000\,\mathrm{N/rad}$.

Acknowledgments

This article is dedicated to Giovanna on the double occasion of our thirtieth wedding anniversary and her fiftieth birthday. Thanks are due to the reviewers for helpful and generous suggestions.

References

Alexander, J. C., and Maddocks, J. H. 1988. On the maneuvering of vehicles. *Siam J. Appl. Math.* 48(1):38–51.

Anderson, S. E. (ed.). 1985. *Proc. of the 3rd Int. Conf. on Automated Vehicle Systems*, Stockholm, Sweden.

Borenstein, J., and Koren, Y. 1987. Motion control analysis of a mobile robot. *J. Dynam. Sys. Measurement Control* 109:73–79.

Chen, C.-T. 1987, *Linear System Theory and Design*, Holt, Rinehart and Winston, Inc.

Corless, M. 1993. Control of uncertain nonlinear systems. *J. Dynam. Sys. Measurement Control* 115:362–373.

Cox, I. J., and Wilfong, G. T. 1990. *Autonomous Robot Vehicles*. New York: Springer-Verlag.

D'Andrea-Novel, B., Bastin, G., and Campion, G. 1992 (Nice, France). Dynamic feedback linearization of nonholonomic wheeled mobile robots. *Proc. of the 1992 ICRA Conference*, pp. 2527–2530.

DeSantis, R. M. 1993. Path-tracking for a car-like mobile robot. *1993 ACC Proceedings*, pp. 64–68.

DeSantis, R. M. 1994a. A novel PID for speed and position control. *J. Dynam. Sys. Measurement Control.* In press.

DeSantis, R. M. 1994b. Path-tracking for car-like robots with single and double steering. *IEEE Trans. On Vehicular Technology*. In press.

DeSantis, R. M., and Hurteau, R. 1990. On the motion control of electric AGVs. *Automazione e Strumentazione* 3:137–150.

Ellis, J. R. 1969. *Vehicle Dynamics*. London: London Business Books.

Fenton, R. E., Melocik, G. C., and Olson, K. W. 1976. On the steering of automated vehicles: Theory and experiments. *IEEE Trans. on Automatic Control* AC-21(3)306–314.

Fernandez, C., Gurvits, L., and Li, Z. X. 1991. Foundations of motion planning. *1991 IEEE Int. Conf. in Robotics and Automation.*

Giralt, G. 1988, *Les Robots Mobiles Autonomes*, LAAS, Toulouse, Publication No. 87308.

Hemami, A., Mehrabi, M. G., and Cheng, R. M. H. 1992. A synthesis of an optimal control law for path tracking in mobile robots. *Automatica* 8(2):383–387.

Kanayama, Y., Kimura, Y., Miyazaki, F., and Noguchi, T. 1990 (Cincinnati, OH). A stable tracking control method for an autonomous mobile robot. *Proc. of the 1990 ICRA Conference*, pp. 384–389.

Kane, T. R., and Levinson, D. A. 1985. *Dynamics: Theory and Applications*. New York: McGraw-Hill.

Latombe, J. C. 1991. *Robot Motion Planning*. Boston, Dordrecht, London: Kluwer Academic Publishers.

Lee, A. Y., 1992, A preview steering autopilot control algorithm for four-wheel steering passenger vehicles, *Journal of Dynamic Systems Measurement and Control, Trans ASME*, vol. 114, pp. 401–409.

Matsumoto, N., and Tomizuka, M., 1992, Vehicle lateral velocity and yaw rate control with two independent control inputs, *Journal of Dynamic Systems Measurement and Control, Trans ASME*, vol. 114, pp. 606–613.

Saha, S. K., and Angeles, G. 1989 (Scottsdale, AZ). Kinematics and dynamics of a three-wheeled 2-DOF AGV. *1989 IEEE International Conference on Robotics and Automation*, pp. 1572–1577.

Downloaded from ijr.sagepub.com at ARIZONA STATE UNIV on August 14, 2016

Sampei, M., Tamura, T., Itoh, T., and Nakamichi, M. 1991 (Osaka, Japan). Path-tracking of trailer-like mobile robot. *Proc. of the 1990 ICRA Conference*, pp. 193–198.

Schwartz, J. T., and Yap, C. K. 1987. *Advances in Robotics I: Algorithmic and Geometric Aspects of Robotics*. Hillsdale, NJ: Lawrence Erlbaum Associates.

Shin, D. H., Singh, S., and Lee, J. J. 1992. Explicit path tracking by autonomous vehicles. *Robotica* 16:537–554.

Walsh, G., Tilbury, D., Sastry, S., Murray, R., and Laumond, J. P. 1992. Stabilization of trajectories for systems with nonholonomic constraints. *Proc. of the 1992 ICRA Conference*, pp. 1999–2004.

Downloaded from ijr.sagepub.com at ARIZONA STATE UNIV on August 14, 2016

Definitions

(x, y):	Workspace coordinates of the tractor's guide point.
θ_1, θ_2:	Tractor's, trailer's heading.
Φ:	Trailer's orientation with respect to the tractor.
δ:	Steering angle.
v_u, v_w:	Velocity of the tractor's center of mass (c.o.m.) in tractor-frame coordinates.
Ω_1, Ω_2:	Angular velocities of the tractor and the trailer.
f_{u1}, f_{u2}, f_{u3}:	Longitudinal forces exerted by the tires (of tractor's front and rear axles and trailer's axle, respectively).
$\mathbf{F}_u$:	$[f_{u1} f_{u2} f_{u3}]'$.
f_p:	Scalar control (propulsion).
f_s:	Scalar control (steering).
a:	Distance from tractor's c.o.m. to front axle.
b:	Distance from tractor's c.o.m. to rear axle.
c:	Distance from tractor's rear axle to vertical joint.
d:	Distance from trailer's c.o.m. to vertical joint.
e:	Distance from trailer's axle to c.o.m.
ℓ_1:	$a + b$, or distance from tractor's rear axle to front axle.
ℓ_2:	$d + e$, or distance from trailer's axle to vertical joint.
$g_0, g_{u1}, g_{u2}, g_{u3}, g_p, g_s$:	Scalar functions of x, y, θ_1, and Φ.
$\mathbf{g}_u$:	$[g_{u1} g_{u2} g_{u3}]$.
$\mathbf{q}$:	$[xy\theta_1\Phi]'$: vehicle's configuration vector.
$\mathbf{v}$:	$[v_u v_w \Omega_1 \Omega_2]'$: vehicle's velocity vector.
$\mathbf{a}$:	$[a_u a_w a_{\theta 1} a_\Phi]'$: vehicle's acceleration vector.
$\mathbf{q}_p(s)$:	Assigned path.
$\mathbf{v}_p(s)$:	Assigned velocity profile.
$\mathbf{a}_p(s)$:	Assigned acceleration profile.
$\mathbf{X}$:	$[\mathbf{q}'\mathbf{v}']'$: state of the vehicle.
$\mathbf{X}_d$:	$[\mathbf{q}_d'\mathbf{v}_d']'$: desired state of the vehicle.
$\mathbf{q}_d$:	Desired configuration of the vehicle.
$\mathbf{v}_d$:	Desired velocity of the vehicle.
v_{os}:	Speed offset.
θ_{os}, Φ_{os}:	Heading offsets.
ℓ_{os}:	Lateral offset.
δ_{os}:	Steering offset.
$\mathbf{x}$:	The state of a linear dynamical system.
u_1, u_2:	Scalar controls.
$\mathbf{u}$:	$[u_1 u_2]'$.
$\mathbf{A}, \mathbf{B}$:	Matrices defining a linear dynamical system.
a_{33}, a_{35}:	Scalar entries of $\mathbf{A}$.
$k_{s1}, k_{s2}, k_{s3}, k_{s4}, k_{p1}, k_{p2}$:	Constant scalar gains.
$\mathbf{K}_s$:	$[k_{s1} k_{s2} k_{s3} k_{s4}]$.
p_{11}, p_{12}:	Eigenvalues of a linear differential equation.
r:	Radius of a circle.
$\mathbf{Q}, \mathbf{S}, \mathbf{P}$:	Positive definite matrices.
$q_1, q_2, q_3 q_4$:	Positive scalars.
m_1, m_2:	Tractor's, trailer's mass.
j_1, j_2:	Tractor's, trailer's moment of inertia about c.o.m.
f_{w1}, f_{w2}, f_{w3}:	Lateral forces exerted by the tires (of tractor's front and rear axle and trailer's axle, respectively).
$\mathbf{F}_w$:	$[f_{w1} f_{w2} f_{w3}]'$.
$\mathbf{D}$:	Inertia matrix of the articulated vehicle.
$\mathbf{G}_0\mathbf{G}_1\mathbf{G}_2\mathbf{G}_3\mathbf{G}_4\mathbf{G}_w\mathbf{G}_u\mathbf{G}_p, \mathbf{T}, \mathbf{H}, \mathbf{H}_0$:	Matrix-valued functions used to describe the vehicle's dynamics.
$\beta_1, \beta_2, \beta_3$:	Sideslip angles.
c_1, c_2, c_3:	Stiffness factors.

Downloaded from ijr.sagepub.com at ARIZONA STATE UNIV on August 14, 2016